Stabilization of silicon honeycomb chains by trivalent adsorbates

C. Battaglia[1], H. Cercellier[1], C. Monney[1], M.G. Garnier[1] and P. Aebi[1]

[1] *Institut de Physique, Université de Neuchâtel, CH-2000 Neuchâtel, Switzerland*

PACS 68.65.La – Quantum wires
PACS 68.47.Fg – Semiconductor surfaces
PACS 61.14.Hg – Low-energy electron diffraction (LEED)
PACS 68.37.Ef – Scanning tunneling microscopy (STM)

Abstract. - The atomic structure of self-assembled quasi-one-dimensional Gd chains on Si(111) has been investigated by low-energy electron diffraction and scanning tunneling microscopy. Based on comparison between Gd and Ca chains we show that this Gd induced surface reconstruction belongs to the class of honeycomb chain-channel structures. This clearly demonstrates that, besides monovalent and divalent adsorbates, also trivalent adsorbates such as Gd stabilize silicon honeycomb chains. Consequently silicon honeycomb chains emerge as an universal building block in adsorbate induced silicon surface reconstructions.

Introduction. – Self-assembled atomic chains on silicon surfaces have been the focus of intense research because of their quasi-one-dimensional (1D) electronic properties and their interesting physics. Recently the fluctuation and condensation phenomena at the metal insulator phase transition of the In/Si(111) system could directly be visualized via scanning tunneling microscopy (STM) [1–4]. Competing periodicities in fractionally filled bands lead to the coexistence of different Peierls distortions for the gold induced reconstructions [5–7].

Another important class of 1D systems are the alkali metal (AM=Li, Na, K, Rb, Cs) and Ag induced, insulating (3×1) reconstructions formed by the deposition of 1/3 monolayer (ML) onto the Si(111) surface. The AM/Si(111) systems adopt the so-called honeycomb chain-channel (HCC) structure [8–10] shown in Fig. 1a) which is stabilized by the transfer of one electron from the monovalent AM adsorbate into the Si surface states.

A very similar reconstruction with (3×"2") periodicity is formed by adsorption of alkaline-earth metals (AEM=Mg, Ca, Sr, Ba), where the ×"2" notation stands for a ×2 periodicity along the adsorbate chains but missing coherence between adjacent chains [11]. Due to the divalency of the adsorbate only 1/6 ML, i.e. half the AM coverage, is required to stabilize the HCC structure [12]. At 1/2 ML divalent adsorbates induce a (2×1) phase which was proposed to be formed of π-bonded Seiwatz chains shown in Fig. 1b) [13, 14]. For intermediate coverages, a series of

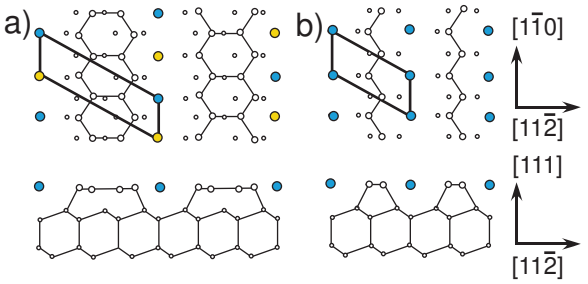

Fig. 1: (Color online) a) Honeycomb chain and b) Seiwatz chain model with adsorbates lying in the channels between the chains. To stabilize the honeycomb chains, monovalent atoms are required to occupy every site in the channels (blue and yellow circles), whereas divalent adsorbates only occupy every second site (blue circles only). Seiwatz chains are stabilized by divalent adsorbates. Open circles are Si atoms. The (3×1) and (2×1) unit cells are also shown.

1D (n×"2") reconstructions, with n taking the values 5, 7 and even 9 depending on the adsorbate, is formed which are considered to be composed of an appropriate combination of honeycomb chains and Seiwatz chains (see Fig. 3 for the 5×"2" case). Similar series of reconstructions were also observed for the divalent rare earth metals (REM) Sm, Eu and Yb [15]. These REMs more commonly occur in the 3+ valence state, but depending on their chemical surrounding the 2+ configuration is occasionally preferred as in this case. Thus up to now, only monovalent and diva-

lent adsorbates were found to stabilize Si reconstructions containing the honeycomb chain building block.
In this letter we focus on trivalent REMs, which exhibit chain structures with (5×"2") periodicity *only*, but whose detailed atomic structure has not been investigated. Combining low-energy electron diffraction (LEED), STM and recent angle-resolved photoemission spectroscopy (ARPES) results [16], we show for the first time that the structure induced by trivalent adsorbates contains the same honeycomb and Seiwatz chains as in the chain reconstructions induced by divalent adsorbates. The use of multiple complementary surface analysis techniques is mandatory in the present case in order to derive a reliable structural model. Based on electron counting we are also able to explain, why only the (5×"2") periodicity is stabilized for trivalent adsorbates.

Experiment. – We choose to investigate the Gd system, since it has recently been demonstrated that predominantly single domain atomic Gd chains can be grown on stepped Si(111) having a slight misscut of 1.1^o towards the $[\bar{1}\bar{1}2]$ direction [17] allowing the use of macroscopic diffraction methods without domain averaging. Qualitatively similar results are expected for the observed (5×"2") reconstruction induced by other trivalent rare-earth metals Dy [18], Er [19] and Ho [20]. Gd was evaporated from a water cooled e-beam evaporator with of flux of 0.5×10^{-4} ML/s at a pressure below 5×10^{-10} mbar onto the clean Si(111)-(7×7) substrate held at 680 ^{o}C. The substrate was heated by passing a direct current along the step direction $[1\bar{1}0]$. Growth and experiments were carried out in an ultra high vacuum chamber with a residual gas pressure of 3×10^{-11} mbar equipped with an Omicron LT-STM and Omicron Spectaleed LEED/Auger optics. For STM measurements we used etched W tips.

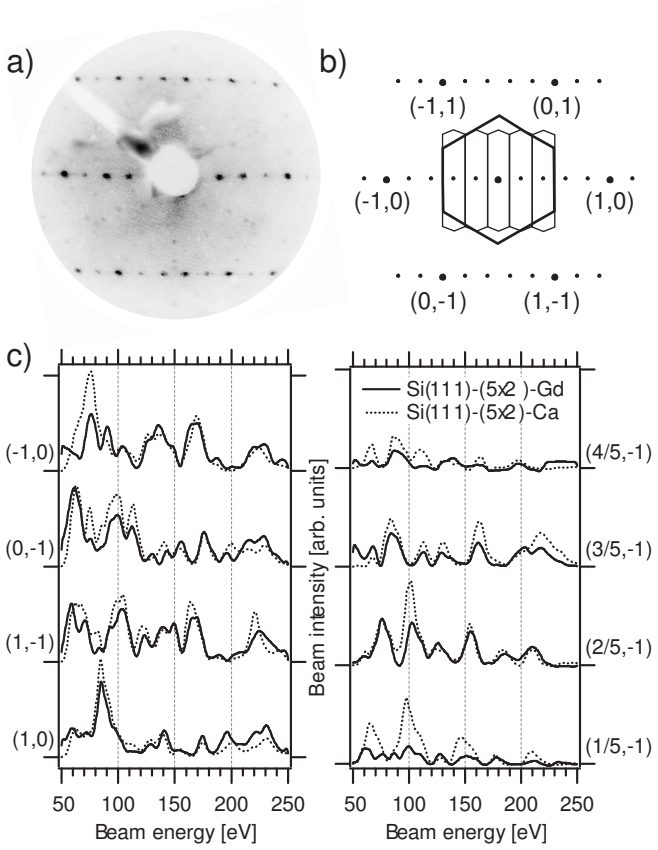

Fig. 2: a) LEED pattern of Si(111)-(5×"2")-Gd at 48 eV. b) Sketch of the 5×1 LEED pattern in reciprocal space with beam indices. In real space the chains are running along the vertical axis. c) Comparison between experimental LEED IV curves of Si(111)-(5×"2")-Gd (full lines) and Si(111)-(5×"2")-Ca (dotted lines).

Results and Discussion. – Figure 2a) shows the LEED pattern of a typical Si(111)-(5×"2")-Gd surface with one dominant domain and insignificant contributions from the two others and the Si(111)-(7×7) reconstruction. Only the (5×1) spots sketched in Fig. 2b) are clearly visible. The ×2 periodicity along the chains manifests itself through faint half-order streaks parallel to the ×5 spots (not shown) observed only at certain energies. Similar streaks were reported in studies of divalent adsorbate systems and explained in terms of a stochastic distribution of adjacent chains with random registry shifts leading to a (5×"2") spot pattern with its characteristic weak half-order streaks [11, 21, 22].
Whereas the LEED spot positions only determine the type of Bravais lattice of the surface structure, i.e. its translational symmetry properties, the point symmetries can be determined by a symmetry analysis of the intensity vs voltage (IV) curves. The threefold symmetry of the unreconstructed Si(111) surface termination is broken by the growth of the chains. Whereas the (0,-1) and (-1,1) beams are still equivalent as for the substrate, the (1,0) beam exhibits a distinctive spectral signature as can be seen from Fig. 2c). Thus only a mirror plane perpendicular to the chains is retained.
To obtain information about the atomic positions we compare LEED IV curves from Si(111)-(5×"2")-Gd to the curves from Si(111)-(5×"2")-Ca in Fig. 2c). IV-LEED fingerprinting has played a crucial role in establishing the equivalence between different AM induced (3×1) HCC reconstructions, since it was recognized that the Si(111)-(3×1)-AM reconstruction is predominantly a substrate reconstruction with a common structure independent of the adsorbate species [23]. Visual inspection of Fig. 2c) already shows that the agreement between the Gd induced and the Ca induced reconstruction containing one honeycomb chain and one Seiwatz chain is surprisingly good. Most peak positions of the Gd chains fall on the same energies as for the Ca chains with comparable relative intensities. To obtain a quantitative measure for the agreement between the two structures we calculated Pendry's R factor R_p [24], which takes into account the peak positions but also the relative intensities between the peaks. For the integral order spots we obtain $R_p = 0.29$. For the fractional order beams we obtain $R_p = 0.35$. These val-

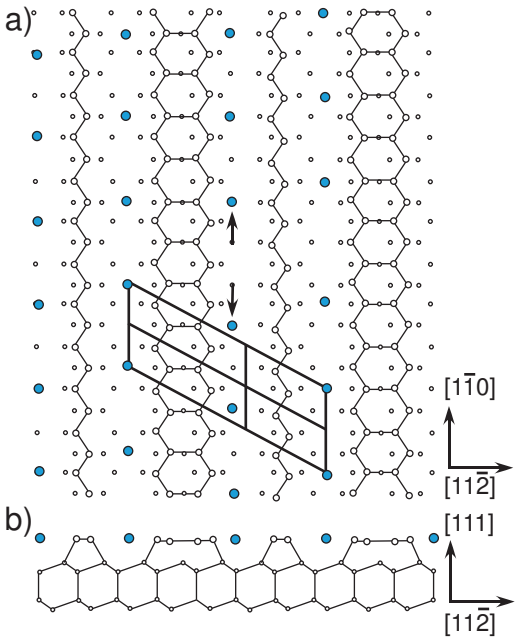

Fig. 3: (Color online) Structural model for the Si(111)-(5×"2")-Gd surface. Open circles are Si atoms, filled blue circles are Gd atoms. The (5×2) unit cell divided into two (3×1) and two (2×1) unit cells is also shown. Arrows indicate a registry shift of the adsorbates in the channel.

ues are similar to $R_p = 0.36$ obtained by Lottermoser [8] comparing theoretical curves to experimental data for the HCC model. The good agreement between the two experiments suggests that both structures share the same structural building blocks. Deviations may be due to the difference in atomic number and the associated scattering characteristics between Gd and Ca, differences in the precise adsorption geometry and coverage.

Adsorbate coverage is an important parameter for the determination of any structural model. The exact amount of Gd at the surface is difficult to determine accurately due to the fact that Gd diffuses into the bulk above 600 ^{o}C [17]. The ideal adsorbate coverage can however be determined when considering the electron count required to stabilize the honeycomb and Seiwatz chains. The HCC structure is known to be stabilized by the donation of one electron per (3×1) unit cell [10,12]. Similarly the Seiwatz chain requires two electrons per (2×1) cell, since it may be stabilized by 1/2 ML of divalent adsorbates. This is consistent with the number of surface states observed in ARPES [25]. The (5×2) unit cell can be thought of as being build from two (3×1) and two (2×1) cells, thus requires six electrons to be stabilized. Since Gd is trivalent, the ideal coverage is two Gd atoms per (5×2) cell or 1/5 ML. This is in agreement with the estimate of 0.2-0.4 ML given in Ref. [17].

The proposed model for the Si(111)-(5×"2")-Gd surface is shown in Fig. 3 consisting of alternating hexagonal honeycomb chains and zig-zag Seiwatz chains made of Si. The adsorbates are expected to form chains in the channels in between. Due to the weak sensitivity of IV-LEED to the adsorbate itself, we can not decide which absorption site is favored. Any structural model must be consistent with results from other experimental techniques. Fig. 4 presents STM images of the Gd chains. The overview a) shows long, parallel chains running along the [1$\bar{1}$0] direction. The separation between the rows is consistent with the ×5 periodicity observed in LEED patterns. High magnification empty and filled state images acquired in the same scan to preserve their mutual registry are shown in Fig. 4b) and c) respectively. The structural model is superimposed. Based on simulated STM images derived from local density approximation (LDA) calculations for the HCC structure [10,12], we identify the dark rows in the empty state image with the location of the honeycomb chains. High intensity in the empty state image is found along the adsorbate channels for both the honeycomb and the Seiwatz chain structure [12,26]. This is easily understood by noticing that the empty orbitals are necessarily located on the adsorbate atom, since it donates its electrons to the silicon chains. The filled state image c) appear as triple rows of protrusions with ×2 periodicity along the rows. The third row located along the Seiwatz chain (marked by S in Fig. 4c) appears to lie slightly lower than the two main rows (marked by H in Fig. 4c), which we identify with the honeycomb chains. In a previous STM study only the two main rows H were resolved [17]. The pairing of protrusions causing the ×2 periodicity along the chains has been found to be rather electronic in origin than geometric [27]. The electrostatic attraction between a positive adsorbate ion and the electrons in the neighboring saturated dangling bonds give rise to such paired protrusions. We also remark that the registry of neighboring chains is correct in our model. Careful inspection of the filled state STM image shows that the honeycomb chain comes in two configurations, either as two parallel rows of protrusions or in a zig-zag configuration, indicated by empty circles in Fig. 4c). Such a registry shift of only one period between the two rows of the honeycomb chain is illustrated by the arrows in Fig. 3 and is simply due to a missing adsorbate and a consecutive shift of all the following adsorbates by one period along the chain direction. The local mixing of these two arrangements with poor long range order is responsible for the ×2 streaks seen in LEED patterns [21]. Furthermore this kind of defect leads to a local charge imbalance. It has been suggested that additional Si adatoms are able to supply electrons that dope the parent chain structure [28] and may be able to compensate for such missing charge. Additional Si atoms are necessarily present since the formation of the HCC structure and consequently also of the (5×"2") structure is accompanied by significant Si mass transport at the surface [29] due to the fact that the Si atom surface density of the (5×"2") structure is not equal to that of Si(111)-(7×7). Although steps may serve as a reservoir for reintegrating ejected Si atoms into the surface, electromigration due to dc current

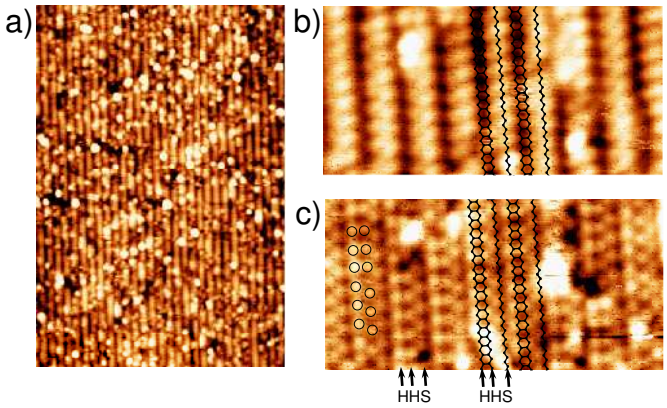

Fig. 4: (Color online) a) STM topography overview (U= 1.9 V), 60 nm × 90 nm, b) and c) high resolution topography of empty (U=1.9 V) and filled states (U=-1.9V), 18 nm × 9 nm, I=0.18 nA. Arrows indicate the location of the honeycomb chain (H) and Seiwatz chain (S). Empty circles mark the two possible configurations of the honeycomb chain caused by a registry shift of the Gd atoms in the adjacent channel as indicated by arrows in Fig. 3.

heating parallel to the steps does not favor the Si atoms to wander towards the steps, resulting in a large number of randomly distributed protrusions on top of the chains.

We now turn to the discussion of recent ARPES results from Si(111)-(5×"2")-Gd [16], which provide additional confirmation for our structural model. At least three semiconducting surface states are observed at binding energies between 1 and 2 eV, whose dispersions, band widths and symmetry properties are very similar to those of the AM and AEM induced (3×1) and (3×"2") reconstructions [30] supporting a honeycomb chain based structure. Furthermore ARPES data for the AEM induced (5×"2") structure resembles the one from the (3×"2") reconstruction. Very weak intensity is observed at the Fermi energy, but has been interpreted as being due to defect states. A small contribution to the spectral weight at the Fermi energy was also observed in the semiconducting Si(111)-(3×"2")-Ca system [21], but was attributed to remaining (7×7) regions of pure silicon. Additionally, prolonged annealing of the Gd induced reconstruction at 680 ^{o}C leads to the nucleation of metallic Gd silicide islands at the expense of the chain reconstruction, which might possibly be responsible for the observed photoelectron signal at the Fermi energy. However, from STM measurements we do not find evidence for a metallic surface state localized on the chains. We conclude that the Gd induced structure is semiconducting and consequently requires an even number of valence electrons per unit cell in agreement with the coverage of two Gd atoms per (5×2) unit cell. Therefore all ARPES results fully support our structural model.

A peculiar experimental finding to be explained is that Gd and other trivalent REMs stabilize chain structures with the (5×"2") symmetry exclusively, whereas the monovalent adsorbates stabilize only the genuine (3× 1) HCC structure and the divalent adsorbates induce a series of (n×"2") reconstructions. Monovalent adsorbates must occupy every site along the channel between the honeycomb chains to satisfy the doping criterion. For lower coverages only parts of the Si(111)-(7×7) are transformed, whereas higher coverages induce different surface structures. The stabilization of Seiwatz chains requiring two electrons per unit cell is not possible. Divalent adsorbates in turn must occupy every second site to satisfy the doping balance. For higher coverages however, additional adsorbates may be incorporated in the channels at the expense of reducing every second honeycomb chain into a Seiwatz chain. For trivalent adsorbates, charge balance requires that every third site in the channel is occupied, if one wants to build a structure exclusively formed by honeycomb chains. This is apparently energetically unfavorable compared to an occupation of every second site, which requires the combination of a honeycomb chain with a Seiwatz chain resulting in the (5×"2") symmetry. The stabilization of a (5×"2") period requires a total of six electrons, a condition easily satisfied by taking two trivalent adsorbates per unit cell. (7×"2") and (9×"2") reconstructions are not observed for the trivalent adsorbates. Consisting of one honeycomb chain and two respectively three Seiwatz chains, they require 10 respectively 14 electrons per unit to be stabilized, a condition which can not be satisfied by trivalent donors. Electron counting thus provides a simple intuitive picture for the occurrence of the various phases.

Conclusion. – Driven by the elimination of dangling bonds and relief of surface stress, silicon surfaces reconstruct in strikingly diverse ways. Among the large variety of adsorbate induced reconstructions, the honeycomb chain emerges as a most stable building block allowing maximum reduction of the surface energy. The fact that only silicon atoms participate in the formation of the honeycomb chains allows a variety of adsorbates to adopt the HCC structure by donating the correct number of electrons to the substrate. Combining the complementary strength of IV-LEED fingerprinting, STM and ARPES, we demonstrated for the first time that next to monovalent and divalent adsorbates, *trivalent adsorbates are also able to stabilize the honeycomb chains*. Based on a intuitive electron counting model, we are further able to explain, why only the (5×"2") symmetry is stabilized by trivalent adsorbates. Our conclusions allow to enlarge the range of honeycomb chain stabilizing adsorbates to the trivalent elements.

* * *

Helpful conversations with Celia Rogero, Laurent Despont, Christian Koitzsch and José A. Martin-Gago are gratefully acknowledged. Skillfull technical assistance was provided by our workshop and electric engineering team. This work was supported by the Fonds National Su-

isse pour la Recherche Scientifique through Div. II and MaNEP.

REFERENCES

[1] G. Lee, J. Guo and E.W. Plummer, *Phys. Rev. Lett.*, **95** (2005) 116103.
[2] S.J. Park, H.W. Yeom, J.R. Ahn and I.-W. Lyo, *Phys. Rev. Lett.*, **95** (2005) 126102.
[3] J. Guo, G. Lee and E.W. Plummer, *Phys. Rev. Lett.*, **95** (2005) 046102.
[4] J.R. Ahn, J.H. Byun, H. Koh, E. Rotenberg, S.D. Kevan and H.W. Yeom, *Phys. Rev. Lett.*, **93** (2004) 106401.
[5] J.N. Crain, A. Kirakosian, K.N. Altmann, C. Bromberger, S.C. Erwin, J.L. McChesney, J.-L. Lin and F.J. Himpsel, *Phys. Rev. Lett.*, **90** (2003) 176805.
[6] J.R. Ahn, P.G. Kang, K.D. Ryang and H.W. Yeom, *Phys. Rev. Lett.*, **95** (2005) 196402.
[7] P.C. Snijders, S. Rogge and H.H. Weitering, *Phys. Rev. Lett.*, **96** (2006) 076801.
[8] L. Lottermoser, E. Landemark, D.-M. Smilgies, M. Nielsen, R. Feidenhans'l, G. Falkenberg, R.L. Johnson, M. Gierer, A.P. Seitsonen, H. Kleine, H. Bludau, H. Over, S.K. Kim and F. Jona, *Phys. Rev. Lett.*, **80** (1998) 3980.
[9] C. Collazo-Davila, D. Grozea and L.D. Marks, *Phys. Rev. Lett.*, **80** (1998) 1678
[10] S.C. Erwin and H.H. Weitering, *Phys. Rev. Lett.*, **81** (1998) 2296
[11] K. Sakamoto, W. Takeyama, H.M. Zhang and R.I.G. Uhrberg, *Phys. Rev. B*, **66** (2002) 165319
[12] G. Lee, S. Hong, H. Kim, D. Shin, J.-Y. Koo, H.-I. Lee and D.W. Moon, *Phys. Rev. Lett.*, **87** (2001) 56104
[13] A.A. Baski, S.C. Erwin, M.S. Turner, K.M. Jones, J.W. Dickinson and J.A. Carlisle, *Surf. Sci.*, **476** (2001) 22
[14] T. Sekiguchi, F. Shimokoshi, T. Nagao and S. Hasegawa, *Surf. Sci.*, **493** (2001) 148
[15] K. Sakamoto, A. Pick and R.I.G. Uhrberg, *Phys. Rev. B*, **72** (2005) 195342 and references cited therein
[16] T. Okuda, T. Tohyama, X.-D. Ma, T. Wakita, A. Harasawa and T. Kinoshita, *J. Electron Spectros. Relat. Phenom.*, **137-140** (2004) 125
[17] A. Kirakosian, J.L. McChesney, R. Bennewitz, J.N. Crain, J.-L. Lin and F.J. Himpsel, *Surf. Sci.*, **498** (2002) L109
[18] I. Engelhardt, C. Preinesberger, S.K. Becker, H. Eisele and M. Dähne, *Surf. Sci.*, **600** (2006) 755-761
[19] P. Wetzel, C. Pirri, G. Gewinner, S. Pelletier, P. Roge, F. Palmino and J.C. Labrune, *Phys. Rev. B*, **56** (1997) 9819
[20] F.J. Himpsel, J.L. McChesney, J.N. Crain, A. Kirakosian, V. Pérez-Dieste, N.L. Abbott, Y.-Y. Luk, P.F. Nealey and D.Y. Petrovykh, *J. Phys. Chem. B*, **108** (2004) 14484
[21] O. Gallus, Th. Pillo, P. Starowicz and Y. Baer, *Europhys. Lett.*, **60** (2002) 903
[22] M. Kuzmin, P. Laukkanen, R.E. Perälä, R.-L. Vaara and I.J. Väyrynen, *Phys. Rev. B*, **71** (2005) 155334
[23] W.C. Fan and A. Ignatiev, *Phys. Rev. B*, **41** (1989) 3592
[24] J. Pendry, *J. Phys. C*, **13** (1980) 937
[25] K. Sakamoto, A. Pick and R.I.G. Uhrberg, *Phys. Rev. B*, **72** (2005) 045310
[26] S. Jeong, J.Y. Lee and M.H. Kang, *Phys. Rev. B*, **68** (2003) 115314
[27] G. Lee and S. Hong and H. Kim and J.-Y. Koo, *Phys. Rev. B*, **68** (2003) 115314
[28] S.C. Erwin, *Phys. Rev. Lett.*, **91** (2003) 206101
[29] A.A. Saranin, A.V. Zotov, V.G. Lifshits, J.-T. Ryu, O. Kubo, H. Tani, T. Harada, M. Katayama and K. Oura, *Phys. Rev. B*, **58** (1998) 3545
[30] T. Okuda, H. Ashima, H. Takeda, K.-S. An, A. Harasawa and T. Kinoshita, *Phys. Rev. B*, **64** (2001) 165312